CFD Letters

Journal homepage:
https://semarakilmu.com.my/journals/index.php/CFD_Letters/index
ISSN: 2180-1363

MHD Casson Fluid Flow in Stagnation-Point over an Inclined Porous Surface

R. Leelavathi [1], V. Seethamahalakshmi[2], D.Vijaya Kumar[3], T. S. Rao[4], G. Venkata Ramana Reddy[4,*], Abayomi Samuel Oke[5]

[1] Department of Mathematics, Andhra Loyola Institute of Engineering and Technology, Vijayawada, 520008, India
[2] Department of Mathematics, PVP Siddartha Institute of Technology, Kanur, Vijayawada, 520007, India
[3] Department of Mathematics, Lakireddy Bali Reddy College of Engineering,Mylavaram – 521230, India
[4] Department of Engineering Mathematics, Koneru Lakshmaiah Education Foundation, Vaddeswaram, 522302, India
[5] Department of Mathematical Sciences, Adekunle Ajasin University, Akungba-Akoko, Nigeria

ARTICLE INFO

Article history:
Received 30 June 2023
Received in revised form 25 July 2023
Accepted 21 August 2023
Available online 1 January 2024

Keywords:
MHD; Stagnation Point; Viscous dissipation; chemical reaction; Thermal radiation

ABSTRACT

Motivated by the need to comprehend and optimize complex fluid flow phenomena in various engineering and industrial applications, this paper investigates the magnetohydrodynamic (MHD) Casson fluid flow characteristics in the vicinity of a stagnation point over an inclined porous surface. The study addresses the interplay of permeability, viscous dissipation, buoyancy, and volumetric heat source, chemical reaction of the diffusion species, thermal slip, and obliqueness at the bounding surface. The governing equations are transformed into a dimensionless form using appropriate similarity transformations. The resulting nonlinear ordinary differential equations are solved numerically using the fourth-order Runge-Kutta method, coupled with the shooting technique as coded into the bvp4c solver of MATLAB 2021a. Findings from this study show that instability arises due to reduced velocity at low permeability, and Biot number enhances the Newtonian cooling at the surface, a requirement for the design of heat exchangers.

1. Introduction

The significance of the non-Newtonian fluids flow in engineering and industrial applications, especially in chemical processes, has been lately piqued. Due to the fact that the exact horizontal or vertical surfaces are not easy to identify in some industrial processes, it becomes necessary to pay some attention to the study of inclined surfaces. Moreover, a little adjustment in the angle of inclination is enough to bring about the required result in these industrial processes. In the industrial process of forming glass, casting metals, and spinning fibres, stretching of surfaces is necessitated. Crane [1] obtained a solution for an incompressible fluid across a stretching surface. Mohapatra *et al.,* [2, 3] have examined the effect of visco-elastic fluid flow on a deformable surface. Oke and Mutuku [4] carried out a comprehensive review of the Eyring-Powell flow in the existence of a magnetic field (MF) and stretching surface under convective heating. Parida *et al.,* [5] have explored the impact of viscous dissipative nanofluid flow over a deformable sheet. They noticed that

[*] *Corresponding author.*
E-mail address: gvrr1976@gmail.com (G. Venkata Ramana Reddy)

https://doi.org/10.37934/cfdl.16.4.6984

strengthening of chemical reactiveness leads to reduced fluid motion and mass concentration. In solar thermal collectors and refrigeration, the simultaneous study of heat transfer and mass transport in MHD flow on stretched surfaces finds significance.

Many scholars work on fluid models such as the viscoelastic, Casson fluid, Oldroyd fluid and nanofluid models [6 - 18]. Shehzad *et al.,* [19] expanded Rahman's [20] work to the Jeffrey fluid model. Swain and Senapati [21] investigated mass transport on MHD flow past a vertical plate that started spontaneously. Chaim [22] and Abel *et al.,* [23] studied dissipative flow in an MHD flow over a sheet stretching. Thorough research on the nature of dissipative flows in various geometrical surface structures is also a subject of interest [24 - 31]. Importantly, the outcomes show that chemical reaction has a significant effect on flows. The study of heat transport along an inclined porous surface is crucial in various industries such as paper production, glass manufacturing, plastic film production, wire drawing, and more. Juma *et al.,* [32] explored the MHD Williamson fluid flow across a rotating inclined plane.

This research presents a novel investigation into the magnetohydrodynamic (MHD) Casson fluid flow near a stagnation point over an inclined porous surface, addressing a significant research gap in the field of fluid dynamics. The originality of this paper lies in its comprehensive exploration of complex fluid flow phenomena, including the intricate interplay of permeability, viscous dissipation, buoyancy effects, volumetric heat source, chemical reactions of diffusing species, thermal slip, and surface inclination. While existing literature has provided foundational insights into MHD flows and porous media, our study advances the field by uniquely combining these factors. The practical significance of this research is underscored by its relevance to heat exchanger design and performance optimization in various industrial processes. By employing numerical techniques and innovative mathematical transformations, we bridge the existing knowledge gap, providing a clear roadmap for further research in this domain and offering valuable insights into fluid dynamics, which have critical implications for engineering and industrial applications. This work not only enhances our understanding of complex fluid flow but also serves as a foundation for future investigations in optimizing fluid dynamics in porous media and industrial systems.

2. Mathematical Formulation

A 2-D MHD Casson fluid free-convective incompressible flow towards an inclined nonlinear porous expanding sheet is studied (see Figure 1). Inclination of the surface at angle α $(0 \leq \alpha \leq \pi/2)$. The flow is in the upper region $y > 0$ under a normal uniform MF of strength$B(x) = \frac{B_0}{\sqrt[3]{x}}$. The surface is undergoing a nonlinear stretching with velocity $u_w(x) = c\sqrt[3]{x}$, where a stretching intensity is. The flow arises in fluids near a stagnation point attributable to relations of gravity and density difference down to diffusion of chemical species, thermal energy diffusion, and stretching of the inclined sheet. The temperature T and concentration C have values T_w and C_w precisely on the surface. The characteristics of thermal radiation are investigated through convective heating involving temperature T_f and a heat exchange factor h_f that is inversely proportional to x. However, the temperature T_∞ and mass partition C_∞ for nano-liquids at the free stream are as illustrated in Figure 1. The mathematical representation of the Casson fluid is expressed as follows [33]:

$$\tau_{ij} = \begin{cases} 2\left(\mu_b + \left(\dfrac{P_y^2}{2\pi_0}\right)^{\frac{1}{2}}\right)e_{ij}, & \pi_0 > \pi_c \\ 2\left(\mu_b + \left(\dfrac{P_y^2}{2\pi_c}\right)^{\frac{1}{2}}\right)e_{ij}, & \pi_0 < \pi_c \end{cases} \tag{1}$$

where τ_{ij} represents the $(i,j)^{th}$ stress tensor component, p_y indicates fluid's yield stress, μ_B is synthetic absolute fluids' viscosity, and π is the component of the deformation rate multiplied by itself, which is defined as $\pi_0 = e_{ij}e_{ij}$, and e_{ij} is $(i,j)^{th}$ deformation rate, and π_c is considered as the critical value of π_0.

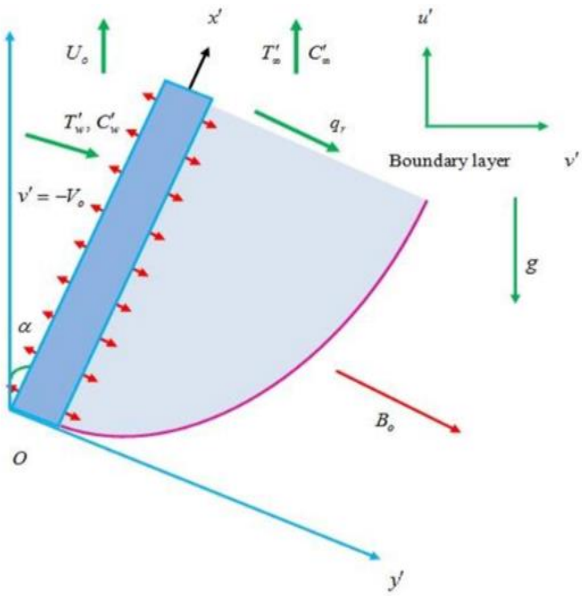

Fig. 1. Geometry of the problem

The governing equations for flow separation and Boussinesq approximation were specified by Eq. (2) to Eq. (5), which are based on Reddy *et al.,* [33]:

$$\frac{\partial u}{\partial x} + \frac{\partial v}{\partial y} = 0 \tag{2}$$

$$u\frac{\partial u}{\partial x} + v\frac{\partial u}{\partial y} = \nu\left(1 + \frac{1}{\beta}\right)\frac{\partial^2 u}{\partial y^2} - \left[\frac{\sigma B_0^2}{\rho} + \frac{\nu}{K}\right]u + [g\beta_T(T - T_\infty) + g\beta_C(C - C_\infty)]\,cos(a) \tag{3}$$

$$u\frac{\partial T}{\partial x} + v\frac{\partial T}{\partial y} = \frac{k}{\rho Cp}\frac{\partial^2 T}{\partial y^2} - \frac{\mu}{\rho Cp}\left(1 + \frac{1}{\beta}\right)\left(\frac{\partial u}{\partial y}\right)^2 - \frac{1}{\rho Cp}\frac{\partial q_r}{\partial y} + \frac{Q_1}{\rho Cp}(T - T_\infty) \tag{4}$$

$$u\frac{\partial C}{\partial x} + v\frac{\partial C}{\partial y} = D_M\frac{\partial^2 C}{\partial y^2} - Kr'(C - C_\infty) \tag{5}$$

with the boundary conditions:

$$\begin{cases} u = u_w(x), v = v_w, -k\frac{\partial T}{\partial y} = h_f(x)(T_w - T), C = C_\infty + bx, \text{at } \ y = 0 \\ \qquad\qquad u \to 0, T \to T_\infty, C \to C_\infty \text{ as } \ \mathrm{y} \to \infty \end{cases} \tag{6}$$

where velocity in x and y- planes are u and v, K is the porous medium specification, β is Casson fluid parameter, g is gravity acceleration, Kr is chemical reaction parameterν is fluid kinematic viscosity, ρ is fluid density, σ is electrical conductivity, a is angle of inclination, Cp is specific heat, DM is molecular diffusion, q_r is radiative heat flux, and Q_1 is heat absorption.

By taking into account the Rosseland dispersion for the q_r [29], it is possible to minimise the viability condition Eq. (4), and we get.

$$q_r = -\frac{4\sigma *}{3k *}\frac{\partial T^4}{\partial y} \tag{7}$$

where σ^* is Stefan-Boltzmann consistent and k^* is the mean ingestion.

For a very small temperature in the stream, Taylor's method calls for expanding T^4 around T and avoiding higher terms, we get:

$$T^4 = 4T_\infty^3 T - 3T_\infty^4 \tag{8}$$

Heat flux can be estimated as

$$\frac{\partial q_r}{\partial y} = -\frac{16T_\infty^3\sigma *}{3k *}\frac{\partial^2 T}{\partial y^2} \tag{9}$$

Using Eq. (9) in energy Eq. (4), one can get:

$$u\frac{\partial T}{\partial x} + v\frac{\partial T}{\partial y} = \frac{k}{\rho Cp}\frac{\partial^2 T}{\partial y^2} + \frac{\mu}{\rho Cp}\left(1+\frac{1}{\beta}\right)\left(\frac{\partial u}{\partial y}\right)^2 + \frac{1}{\rho Cp}\left(\frac{16T_\infty^3\sigma^*}{3k *}\right)\frac{\partial^2 T}{\partial y^2} + \frac{Q_1}{\rho Cp}(T - T_\infty) \tag{10}$$

The below-mentioned similarity transformation reduces Eq. (2), (3), (10), and Eq. (5):

$$\eta = c\nu^{\frac{1}{2}}yx^{-\frac{1}{3}}, \psi = x^{\frac{2}{3}}c^{\frac{1}{2}}\nu^{\frac{1}{2}}f(\eta)$$
$$\theta(\eta) = \frac{T - T_\infty}{T_w - T_\infty}, \phi(\eta) = \frac{C - C_\infty}{C_w - C_\infty} \tag{11}$$

The Eq. (3), (5), and Eq. (10) are represented in a dimensionless form by utilizing similarity transformation Eq. (11) for a nonlinear ODE system:

$$(1+\beta^{-1})f''' + \frac{2}{3}ff'' + \left(M + \frac{1}{K}\right)f' + \lambda(\theta + N\phi)\cos(a) = 0 \tag{12}$$
$$\left(1+\frac{1}{\beta}\right)Ecf''^2 + \frac{2}{3}f\theta' - \theta f' + \frac{1}{Pr(1+Nr)''} + PrQ = 0 \tag{13}$$
$$\phi'' - ScKr\phi + \frac{2}{3}Sc(f\phi' - f'\phi) = 0 \tag{14}$$

The appropriate dimensionless version of boundary conditions is given by:

$$f = S, f' = 1, \theta' = -Bi(1-\theta), \phi = 1 \text{ at } \eta = 0$$
$$f' \to 0, \theta \to 0, \phi \to 0 \quad \eta \to \infty \tag{15}$$

The dimensionless constants are

$$M = \frac{\sigma B_0^2}{\rho c}, K = \frac{K_1 c}{\nu x^{\frac{2}{3}}}, \lambda_T = \frac{g\beta_T(T_w - T_\infty)}{c^2 x^{-\frac{1}{3}}}, Re_x = \frac{u_w x}{\nu}, \lambda_C = \frac{g\beta_C(C_w - C_\infty)}{c^2 x^{-\frac{1}{3}}},$$
$$S = \frac{-3v_w x^{\frac{2}{3}}}{2\sqrt{\nu c}}, \lambda = \frac{\lambda_C}{\lambda_T}, Pr = \frac{\rho Cp}{k}, Nr = \frac{16\sigma^* T_\infty^3}{3kk^*}, Q = \frac{Q_1 x^{-\frac{2}{3}}}{c\rho Cp}, Bi = \frac{h_f x^{\frac{1}{3}}\sqrt{\nu}}{kc^{\frac{1}{2}}},$$
$$\frac{1}{Sc} = \frac{D_M}{\nu}, Kr = \frac{Kr'}{cx^{-\frac{2}{3}}}, Ec = \frac{c^2 x^{\frac{2}{3}}}{Cp(T_w - T_\infty)} \tag{16}$$

The three primary physical qualities taken into consideration are the friction force (Cf), Nusselt number (Nu), and Sherwood number (Sh):

$$Cf = \frac{\mu}{\rho u_w^2}\left(\frac{\partial u}{\partial y}\right)_{y=0}, Nu = \frac{x}{(T_w - T_\infty)}\left(\frac{\partial T}{\partial y}\right)_{y=0}, Sh = \frac{x}{(C_w - C_\infty)}\left(\frac{\partial C}{\partial y}\right)_{y=0} \tag{17}$$

Substituting Eq. (11) into Eq. (17) to obtain the final dimensional form:

$$C_f = \sqrt{Re_x} f''(0), Nu = -\sqrt{Re_x}\,\theta'(0), Sh = -\sqrt{Re_x}\,\phi'(0) \tag{18}$$

3. Method of Solution

Eq. (12) - (14) alongside the conditions Eq. (15) are solved by shooting method along with BVP4C with the help of MATLAB 2017a numerically. Eq. (8) - (10) have been converted to a set of 1storder ODE by taking following substitutions:

$$f = h_1, f' = h_2, f'' = h_3, \theta = h_4, \theta' = h_5, \phi = h_6, \phi' = h_7 \tag{19}$$

The transformed equations are as follows:

$$h_3' = \frac{\left[\left(M + \frac{1}{K}\right)h_2 - \frac{2}{3}h_1 h_3 + \frac{1}{3}h_2^2 - \lambda\cos(a)\,(h_4 + Nh_6)\right]}{\left(1 + \frac{1}{\beta}\right)},$$
$$h_5' = \frac{Pr\left(-Qh_4 - \frac{2}{3}h_1 h_5 + h_1 h_4 - Ech_3^2\right)}{1 + Nr},$$
$$h_7' = KrSch_6 - \frac{2}{3}Sch_1 h_7 + Sch_2 h_6,$$

with;

$h_1 = S, h_2 = 1, h_5 = -Bi(1 - h_4), h_6 = 1$ at $\eta = 0.$
$h_2 \to 0, h_4 \to 0, h_6 \to 0 \text{as} \eta \to \infty$

The initial guess values to unknowns h_3, h_5 and h_7 are provided at $\eta = 0$. The numerical procedure adopts a uniform step length $\delta = 0.001$ and an error tolerance of 0.001. See Oke [34] for more numerical methods.

4. Validation

It is important to validate the solutions obtained in this study to ascertain the reliability of the results. To do this, we compare our results with the results of Rashidi *et al.,* [35] and Thumma *et al.,* [36]. The first table (Table 1) is obtained by setting $Pr = 2,\ Q = 0, a = 0, Bi \to \infty, Kr = 0, Ec = 0, K \to \infty, M = 0, Nr = 0$ in our study so that it coincides with that of Rashidi *et al.,* [35] Thumma *et al.,* [36] and the second table (Table 2) is obtained by setting $Nr = 0.5, Sc = 0.78, Kr = 0, S = 0.2, a = \frac{\pi}{4}, Ec = 0, K \to \infty, Pr = 0.71, M = 1$ for varying values of Q. Both tables have shown that there is a good agreement between our results and the existing literature. Hence, we can rely on the solution produced from the numerical approach.

Table 1
$Pr = 2, Q = 0, a = 0, Bi \to \infty, Kr = 0, Ec = 0, K \to \infty, M = 0, Nr = 0$

S	$-f''(0)$		
	Rashidi *et al.,* [35]	Thumma *et al.,* [36]	Presents results
-0.5	0.8736447	0.8736784	0.873635
0	0.6776563	0.6776562	0.677635
0.5	0.5188901	0.5188997	0.518856

Table 2
$Nr = 0.5, Sc = 0.78, Kr = 0, S = 0.2, a = \frac{\pi}{4}, Ec = 0, K \to \infty, Pr = 0.71, M = 1$

	Thumma *et al.,* [36]			Presents results		
Q	$-f''(0)$	$-\theta'(0)$	$-\phi'(0)$	$-f''(0)$	$-\theta'(0)$	$-\phi'(0)$
0.5	-0.6339719	3.4526318	1.3346567	-0.6339679	3.4526252	1.3346542
1	-0.6450595	4.8635878	1.3333765	-0.6450569	4.8635755	1.3333651
1.5	-0.6505565	5.9179405	1.3328534	-0.6505479	5.9179358	1.3328473

5. Results and Discussion

The current work's major objective is to examine the influence of heat and mass transportation on the motion of MHD stagnation-point flow in an inclined stretching porous sheet with variable properties. By combining Runge-Kutta and gunshot procedures, the transformed Eq. (12) through Eq. (14) and the boundary conditions they relate to in Eq. (15) have been mathematically solved. Graphs are utilized to illustrate the behaviour of flow, heat, and mass transport characteristics. These graphs include all flow parameter contributions like Casson parameter (β), magnetic specification (M), suction or injection parameter (S), Radiation parameter (Nr), heat supply parameter (Q), and others.

Figure 2 shows how the Casson parameter (β) impacts the velocity profile. As the β value rises, it is seen that the velocity distributions get smaller. This is because as β increases, the yield stress of the Casson fluid parameter decays increasing the rate of plastic dynamic fluid flow. The velocity is reduced when the plastic's absolute viscosity rises, causing fluid flow resistance. Figures 3–4 illustrate the importance of the Schmidt number (Sc) and the chemical reaction parameter (Kr) on the concentration proportion. The concentration profiles degenerate when both Sc and Kr are present in significant amounts. Increasing chemical reaction increases the usage of the reactants thereby reducing the concentration. Figure 5 exhibits the response of dimensionless velocity profiles to M.

Strengthening M values promotes diminution in fluid flow. Physically, M corresponds to Lorentz force as a consequence of which greater values of M enhance Lorentz force and this force is one type of resistive force acting against the motion of the fluid therefore fluid velocity decreases. The impact of the porosity parameter (K) on the velocity profile is seen in Figure 6. A decrease in fluid velocity contour is observed in response to an increase in K. The fluid penetration is extremely slow due to the Casson nanoparticles' random mixing and the imposed magnetic field's strength. Physically, the porous media allows fluid particles to travel within the boundary layer, but the yield exhibiting the fluid's plastic dynamic viscosity slows their motion. Figure 7 exhibits the velocity distribution on α. In each of the figures, the velocity profiles decline asymptotically to zero at the free stream. It can be observed that increasing the angle of inclination has an influence(α). Raising the angle, velocity decreases and hence the buoyancy force decreases and concomitantly velocity decreases.

Positive *Bi* physically supports Newtonian cooling, and its effects on the temperature profiles are shown in Figure 8. As a result of the increased Newtonian cooling, heat transfers from the wall into the fluid, and an increase in Bi raises the temperature. It is also noticed that at a value of Bi=0.1, the temperature is quite low because of the solid surface's poor conductivity. The effect of the electromagnetic radiation variable Nr on the temperature distributions is highlighted in Figure 9. The fluid temperature seems to rise with a high Nr value. Thermal engineering can benefit from this as it helps the fluid's thermal condition. Figure 10 shows that the heat source parameter raises the flow temperature. Subsequently, the thermal boundary layer thickens. Thermal power tends to increase as the heat source increases. The effect of the Eckert number on temperature profiles is shown in Figure 11. As Ec increases, the temperature increases. Clearly, Ec denotes the intensity of Ohmic heating, and a higher Ec indicates more Ohmic heating strength. As a result, heat dissipation improves, and the fluid temperature rises.

Comparisons of the skin friction coefficient for MHD Casson fluid free-convective stagnation-point flow near an inclined non-linear stretching sheet surrounded by a permeable media are carried out to validate the contemporary effects and confirm the veracity of the existing evaluation. Concerning the findings of Rashidi *et al.,* [27], Table 1 compares the skin friction coefficient. The results shown in this table show that there is a good deal of consistency between them and that the skin friction coefficient reduces with the suction parameter's values increase. From Table 2, excellent agreement is between the results from Thumma *et al.,* [29] and our recent findings. The skin friction is increased, and the Sherwood number falls as a result of the heat source parameter Q, whereas the Nusselt number shows the opposite pattern. Table 3 shows the : Variation of physical parameters on Sf, Nu and Sh.

Table 3
Variation of physical parameters on Sf, Nu and Sh

Sc	S	Kr	M	K	α	Bi	Nr	Q	Ec	Sf	Nu	Sh
0.2	0.5	0.5	1	1	$\pi/4$	0	1	1	0	0.646698	0.07541	0.582091
0.3										0.659454	0.075865	0.695983
0.6										0.689958	0.077175	1.05006
0.8										0.701522	0.077728	1.22987
0.8	0.3	0.5	1	1	$\pi/4$	0	1	1	0	0.662524	0.073366	1.15831
	0.5									0.701522	0.07541	1.22987
	0.8									0.741482	0.077379	1.305353
	1									0.782189	0.079232	1.384657
0.8	0.5	0.3	1	1	$\pi/4$	0	1	1	0	0.881848	0.070377	1.099622
		0.5								0.887386	0.070583	1.205881
		0.8								0.891803	0.070847	1.300301
		1								0.895481	0.071202	1.386315
0.8	0.5	0.5	1	0.5	$\pi/4$	0	1	1	0	0.887386	0.055164	1.1584
			2							1.043394	0.060757	1.171517
			3							1.179926	0.065976	1.187023
			4							1.30248	0.070847	1.205881
0.8	0.5	0.5	1	0.3	$\pi/4$	0	1	1	0	0.701522	0.060757	1.171517
				0.5						0.767814	0.070847	1.205881
				0.8						0.887386	0.07392	1.221132
				1						1.179926	0.07541	1.22987
0.8	0.5	0.5	1	0.5	0	0	1	1	0	0.824009	0.061082	1.181243
					$\pi/6$					0.852647	0.070847	1.205881
					$\pi/4$					0.887386	0.071942	1.210419
					$\pi/2$					1.060038	0.072738	1.214082
0.8	0.5	0.5	1	0.5	0	0	1	1	0	0.829596	0.070847	1.205881
						0				0.84189	0.113268	1.210603
						0				0.85944	0.142587	1.2135
						0				0.887386	0.164293	1.2155
0.8	0.5	0.5	1	0.5	0	0	0	1	0	0.894326	0.073855	1.203368
							0			0.89616	0.074633	1.203864
							0			0.898346	0.075551	1.204272
							0			0.900987	0.076649	1.204613
0.8	0.5	0.5	1	0.5	0	0	0	0	0	0.901985	0.076526	1.199659
								0		0.910457	0.079859	1.200386
								0		0.915914	0.082037	1.201435
								0		0.919722	0.083581	1.203069
0.8	0.5	0.5	1	0.5	0	0	0	0	0	0.869909	0.063151	1.205881
									0.01	0.878418	0.066905	1.206031
									0.1	0.886546	0.070479	1.207476
									0.2	0.887386	0.070847	1.208978

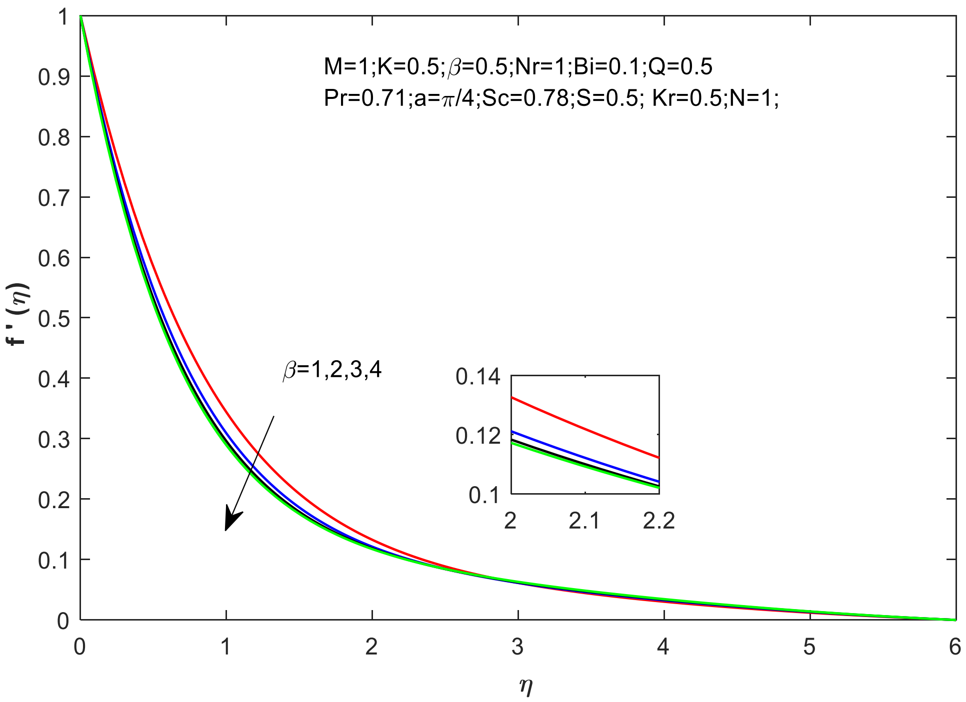

Fig. 2. Velocity response to β

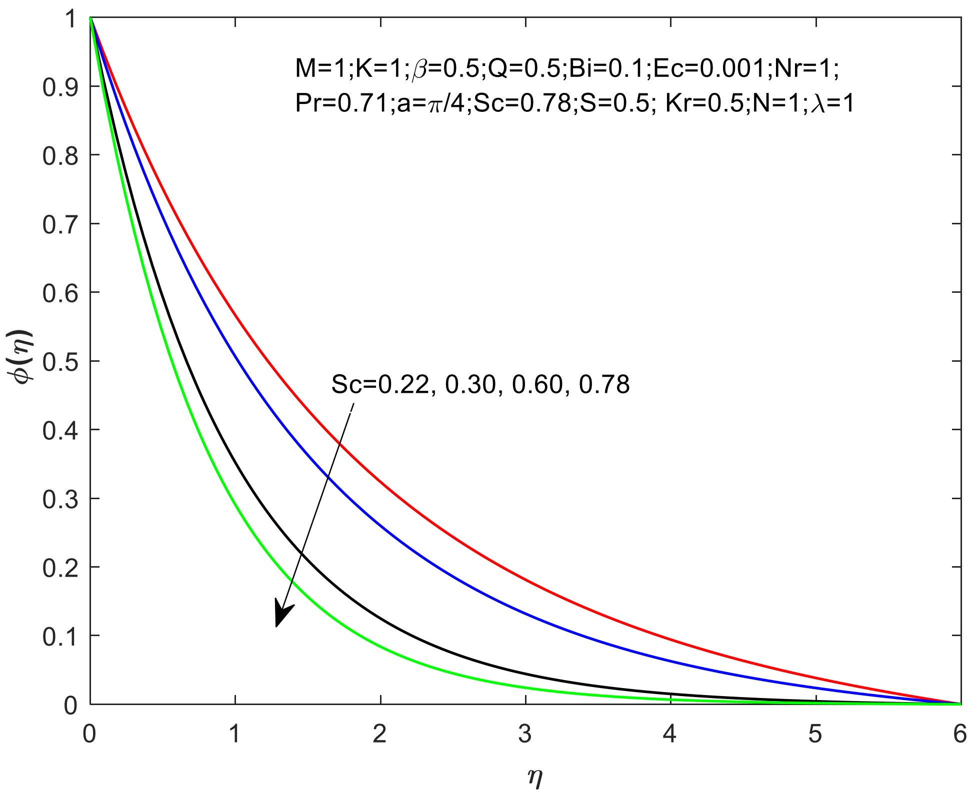

Fig. 3. Concentration response to Sc

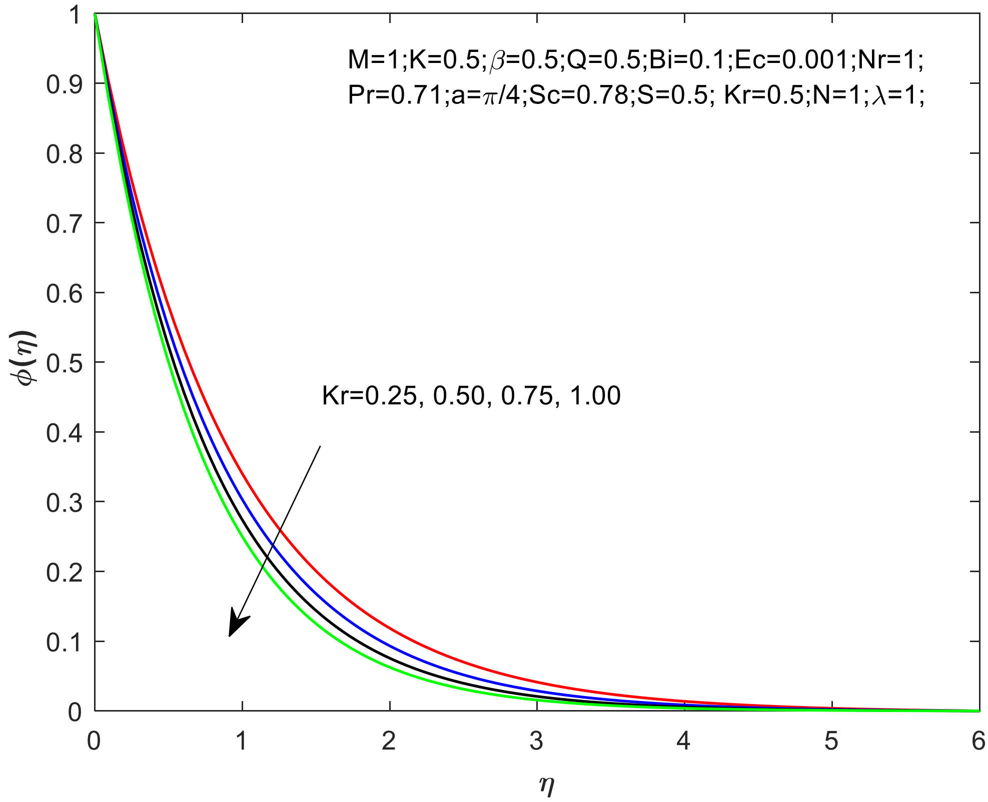

Fig. 4. Concentration response to Kr

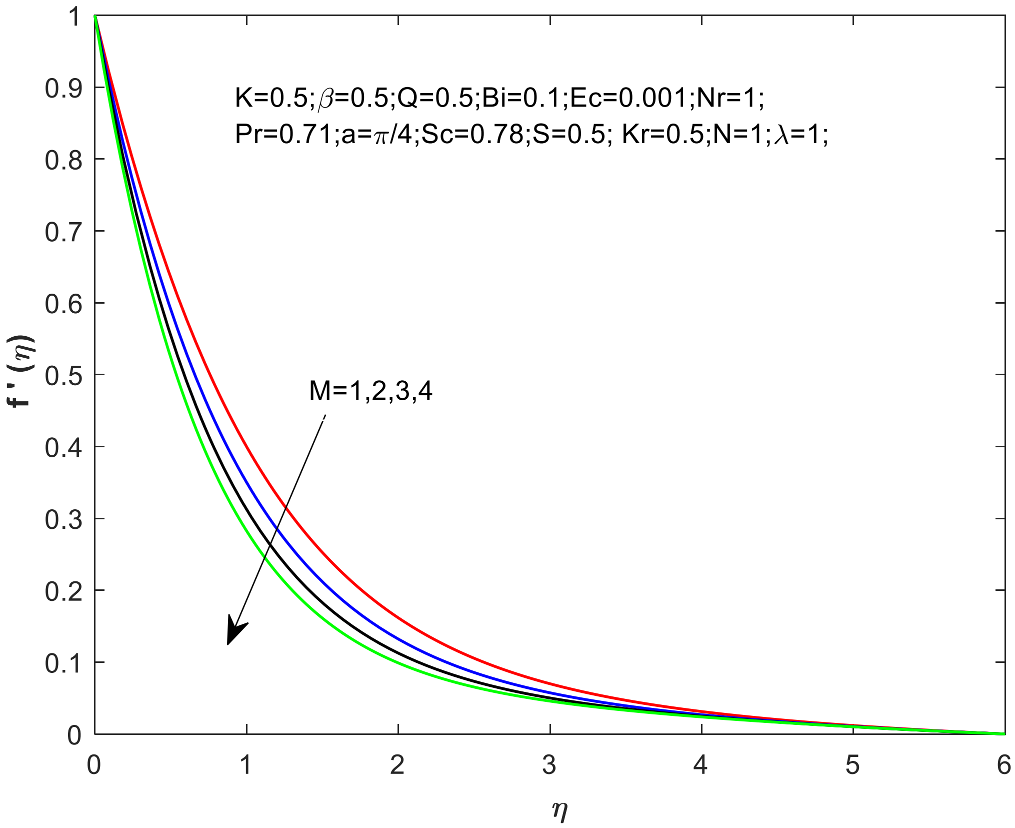

Fig. 5. Velocity response to M

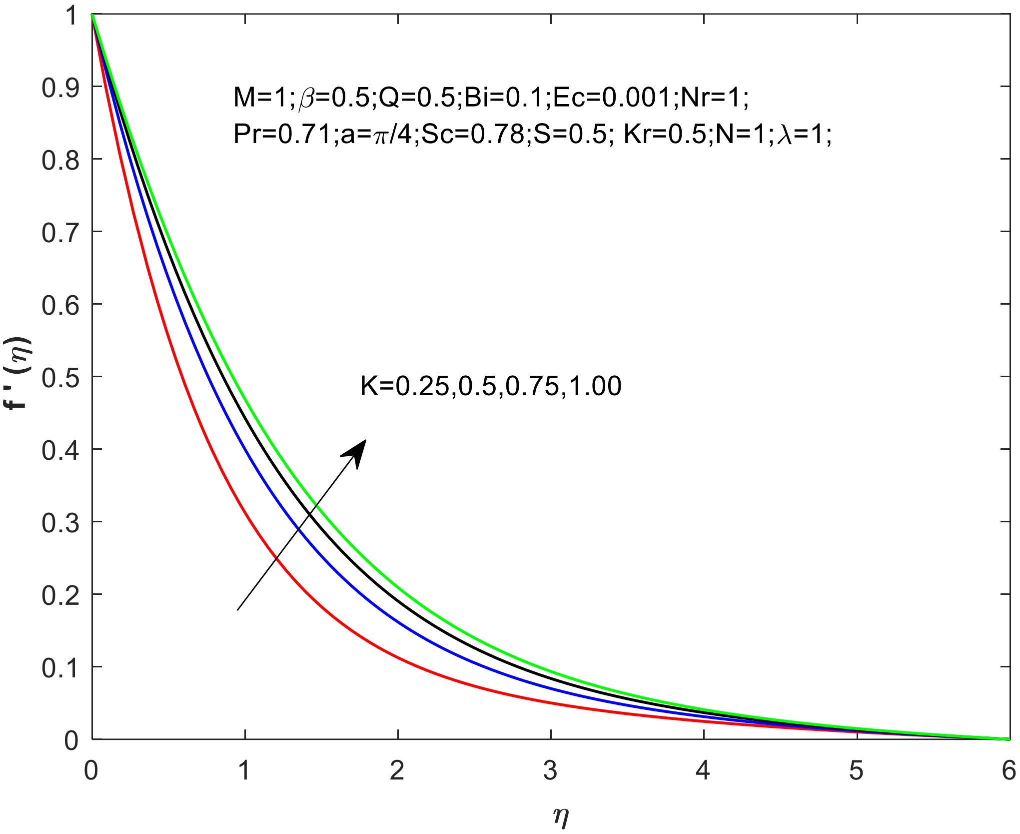

Fig. 6. Velocity response to K

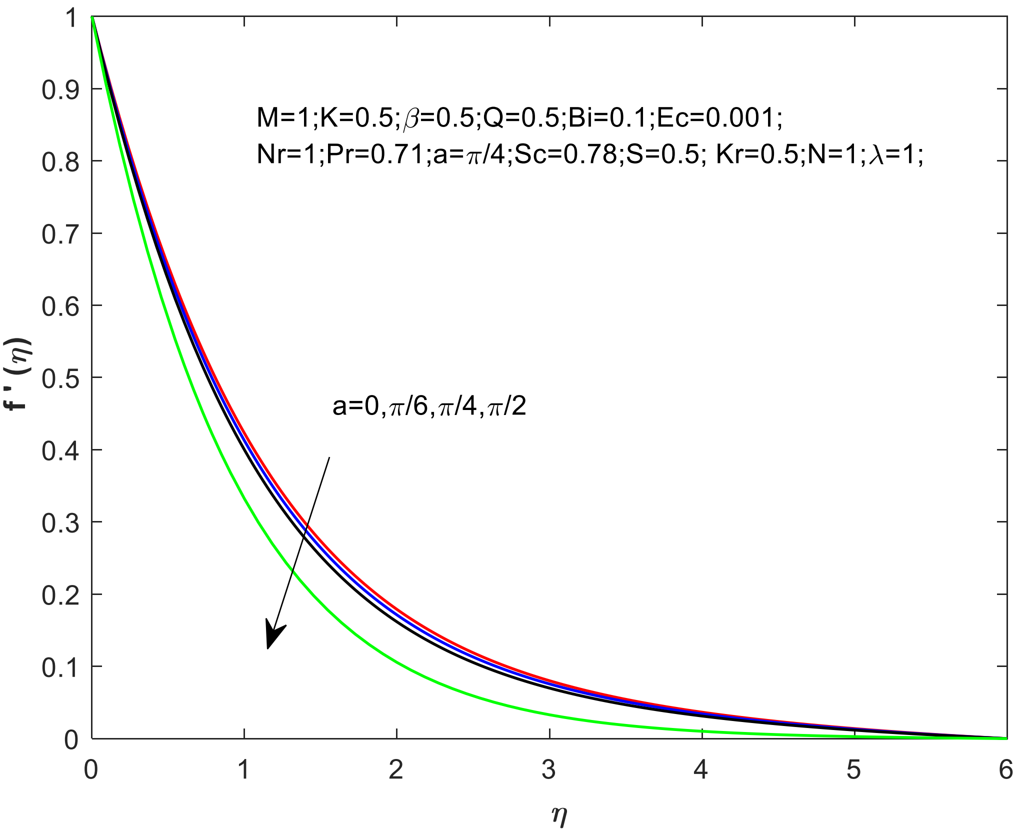

Fig. 7. Velocity response to angle of inclination

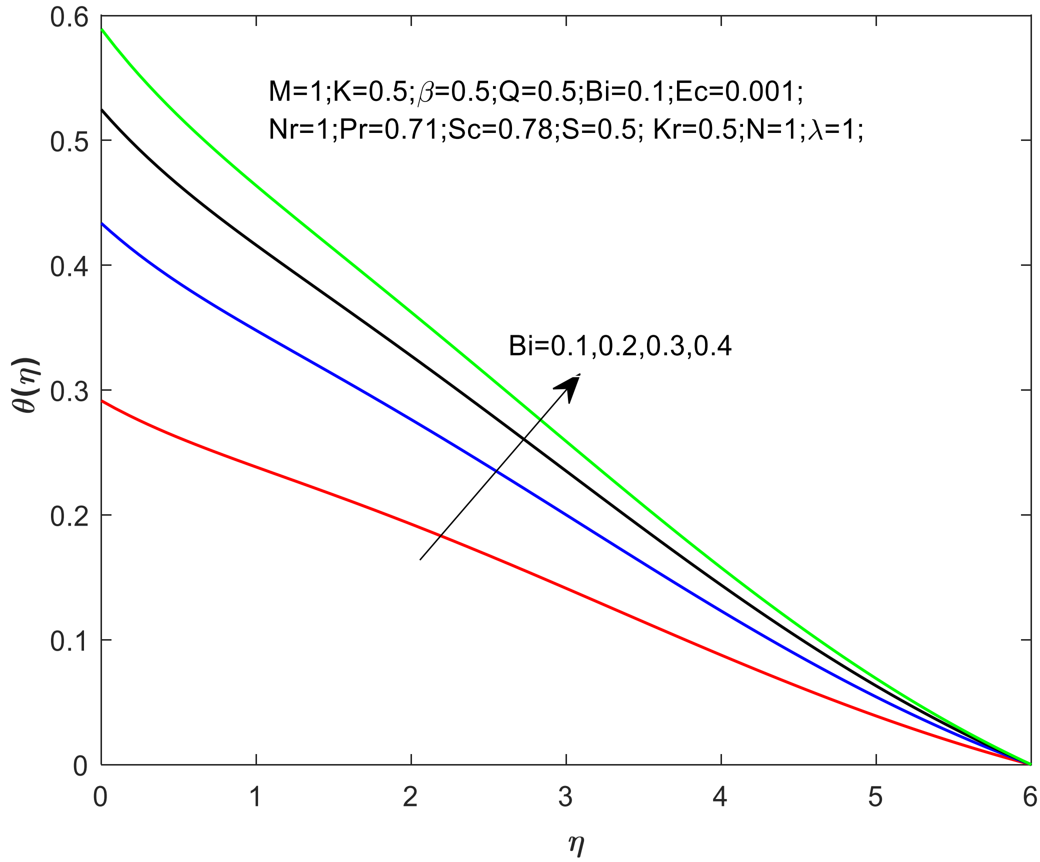

Fig. 8. Temperature response to Bi

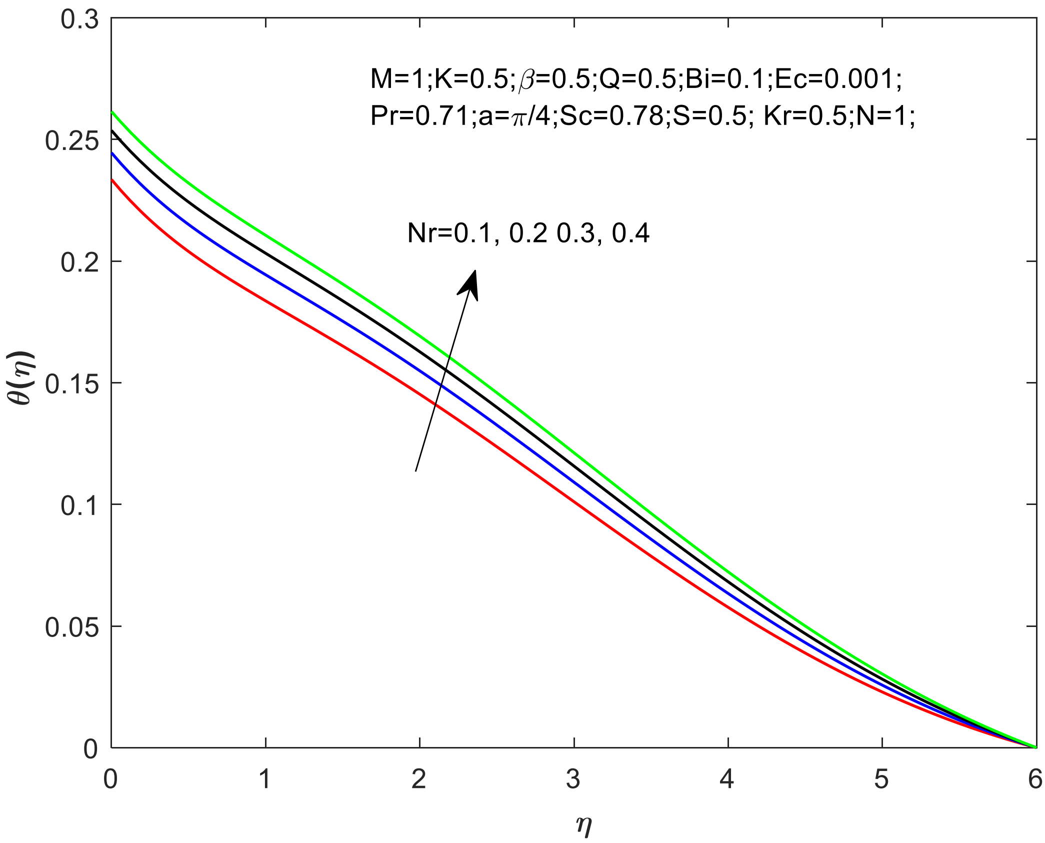

Fig. 9. Response of temperature to Nr

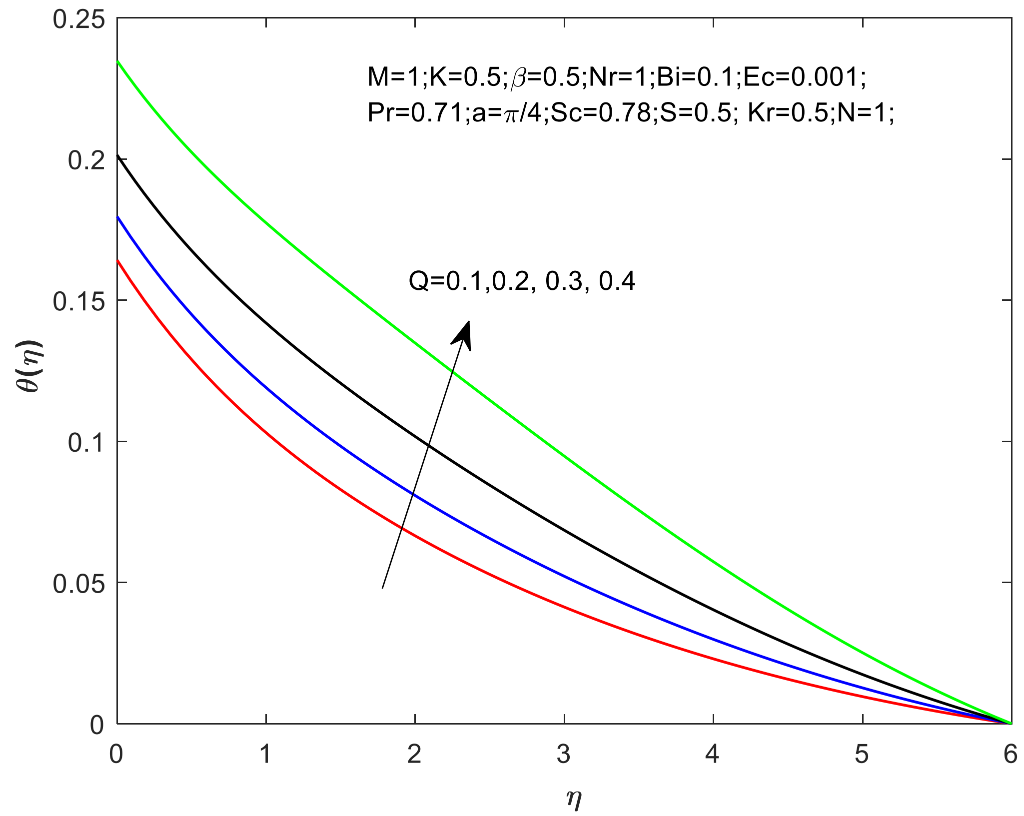

Fig. 10. Response of temperature to Q

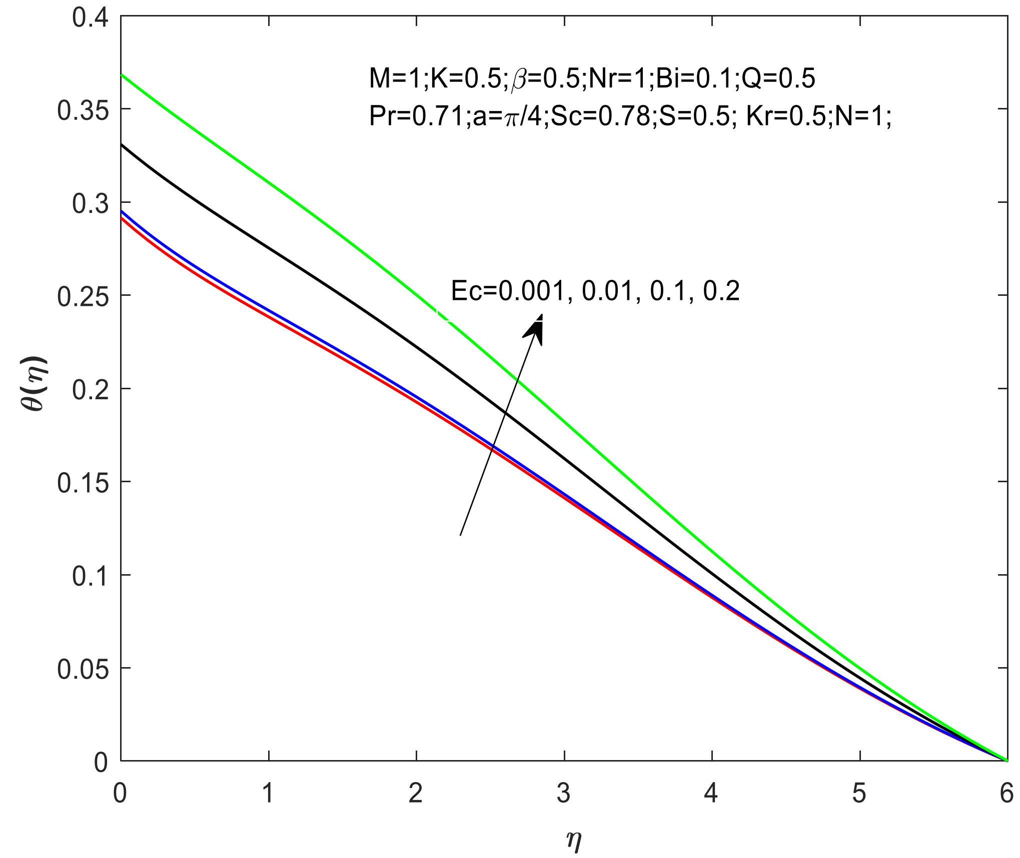

Fig. 11. Response of temperature to Ec

6. Conclusion

Below are the conclusion from this study:

i. Oblique plate reduces the significance of medium permeability and MF causes a reduction in velocity.
ii. Nonnegative Biot number leads to enhancement in fluid temperature.
iii. Reduced permeability causes a drop in velocity at the wall, leading to instability in flow laminarity while high permeability raises the skin friction.
iv. Velocity decreases with increasing Casson fluid flow.
v. Due to the positivity of the heat transfer coefficient and mass transfer coefficient, the wall surface experiences cooling and a reduction in the solutal deposit. Thus, the conclusion finds application in heat exchanger design.

References

[1] Crane, Lawrence J. "Flow past a stretching plate." *Zeitschrift für angewandte Mathematik und Physik ZAMP* 21 (1970): 645-647. https://doi.org/10.1007/BF01587695
[2] Mahapatra, T. Ray, S. Dholey, and A. S. Gupta. "Heat transfer in oblique stagnation-point flow of an incompressible viscous fluid towards a stretching surface." *Heat and mass transfer* 43, no. 8 (2007): 767-773. https://doi.org/10.1007/s00231-006-0116-8
[3] Mahapatra, T. Ray, S. Dholey, and A. S. Gupta. "Momentum and heat transfer in the magnetohydrodynamic stagnation-point flow of a viscoelastic fluid toward a stretching surface." *Meccanica* 42 (2007): 263-272. https://doi.org/10.1007/s00231-006-0116-8
[4] Oke, Abayomi S., and Winifred N. Mutuku. "Significance of viscous dissipation on MHD Eyring–Powell flow past a convectively heated stretching sheet." *Pramana* 95, no. 4 (2021): 199. https://doi.org/10.1007/s00231-006-0116-8
[5] Parida, B. C., B. K. Swain, and N. Senapati. "MASS TRANSFER EFFECT ON VISCOUS DISSIPATIVE MHD FLOW OF NANOFLUID OVER A STRETCHING SHEET EMBEDDED IN A POROUS MEDIUM." *Journal of Naval Architecture & Marine Engineering* 18, no. 1 (2021). https://doi.org/10.1007/s00231-006-0116-8
[6] Turkyilmazoglu, M. "Exact analytical solutions for heat and mass transfer of MHD slip flow in nanofluids." *Chemical Engineering Science* 84 (2012): 182-187. https://doi.org/10.1007/s00231-006-0116-8
[7] Hayat, T., S. A. Shehzad, and A. Alsaedi. "Soret and Dufour effects on magnetohydrodynamic (MHD) flow of Casson fluid." *Applied Mathematics and Mechanics* 33 (2012): 1301-1312. https://doi.org/10.1007/s00231-006-0116-8
[8] Rani, K. Sandhya, G. Venkata Ramana Reddy, and Abayomi Samuel Oke. "Significance of Cattaneo-Christov Heat Flux on Chemically Reacting Nanofluids Flow Past a Stretching Sheet with Joule Heating Effect." *CFD Letters* 15, no. 7 (2023): 31-41. https://doi.org/10.37934/cfdl.15.7.3141
[9] Alipour, Navid, Bahram Jafari, and Kh Hosseinzadeh. "Optimization of wavy trapezoidal porous cavity containing mixture hybrid nanofluid (water/ethylene glycol Go–Al2O3) by response surface method." *Scientific Reports* 13, no. 1 (2023): 1635. https://doi.org/10.1038/s41598-023-28916-2
[10] Akbari, Shahin, Shahin Faghiri, Parham Poureslami, Khashayar Hosseinzadeh, and Mohammad Behshad Shafii. "Analytical solution of non-Fourier heat conduction in a 3-D hollow sphere under time-space varying boundary conditions." *Heliyon* 8, no. 12 (2022). https://doi.org/10.1016/j.heliyon.2022.e12496
[11] Hosseinzadeh, S., Kh Hosseinzadeh, A. Hasibi, and D. D. Ganji. "Thermal analysis of moving porous fin wetted by hybrid nanofluid with trapezoidal, concave parabolic and convex cross sections." *Case Studies in Thermal Engineering* 30 (2022): 101757. https://doi.org/10.1016/j.csite.2022.101757
[12] Bachok, Norfifah, Siti Nur Nazurah Tajuddin, Nur Syazana Anuar, and Haliza Rosali. "Numerical Computation of Stagnation Point Flow and Heat Transfer over a Nonlinear Stretching/Shrinking Sheet in Hybrid Nanofluid with Suction/Injection Effects." *Journal of Advanced Research in Fluid Mechanics and Thermal Sciences* 107, no. 1 (2023): 80-86. https://doi.org/10.37934/arfmts.107.1.8086
[13] Soid, Siti Khuzaimah, Siti Nor Asiah Ab Talib, Nur Hazirah Adilla Norzawary, Siti Suzilliana Putri Mohamed Isa, and Muhammad Khairul Anuar Mohamed. "Stagnation Bioconvection Flow of Titanium and Aluminium Alloy Nanofluid Containing Gyrotactic Microorganisms over an Exponentially Vertical Sheet." *Journal of Advanced Research in Fluid Mechanics and Thermal Sciences* 107, no. 1 (2023): 202-218. https://doi.org/10.37934/arfmts.107.1.202218

[14] Hayat, Tasawar, and Ahmed Alsaedi. "On thermal radiation and Joule heating effects in MHD flow of an Oldroyd-B fluid with thermophoresis." *Arabian Journal for Science and Engineering* 36 (2011): 1113-1124. https://doi.org/10.1007/s13369-011-0066-4

[15] Oke, Abayomi S., Ephesus O. Fatunmbi, Isaac L. Animasaun, and Belindar A. Juma. "Exploration of ternary-hybrid nanofluid experiencing Coriolis and Lorentz forces: case of three-dimensional flow of water conveying carbon nanotubes, graphene, and alumina nanoparticles." *Waves in Random and Complex Media* (2022): 1-20. https://doi.org/10.1080/17455030.2022.2123114

[16] Oke, A. S. "Coriolis effects on MHD flow of MEP fluid over a non-uniform surface in the presence of thermal radiation." *International Communications in Heat and Mass Transfer* 129 (2021): 105695. https://doi.org/10.1016/j.icheatmasstransfer.2021.105695

[17] Oke, A. S. "Theoretical analysis of modified eyring powell fluid flow." *Journal of the Taiwan Institute of Chemical Engineers* 132 (2022): 104152. https://doi.org/10.1016/j.jtice.2021.11.019

[18] Oke, Abayomi Samuel. "Heat and mass transfer in 3D MHD flow of EG-based ternary hybrid nanofluid over a rotating surface." *Arabian Journal for Science and Engineering* 47, no. 12 (2022): 16015-16031. https://doi.org/10.1007/s13369-022-06838-x

[19] Shehzad, S. A., A. Alsaedi, and T. Hayat. "Influence of thermophoresis and Joule heating on the radiative flow of Jeffrey fluid with mixed convection." *Brazilian Journal of Chemical Engineering* 30 (2013): 897-908. https://doi.org/10.1590/S0104-66322013000400021

[20] Rahman, M. M. "Convective flows of micropolar fluids from radiate isothermal porous surfaces with viscous dissipation and Joule heating." *Communications in Nonlinear Science and Numerical Simulation* 14, no. 7 (2009): 3018-3030. https://doi.org/10.1016/j.cnsns.2008.11.010

[21] Swain, Bharat Keshari, and Nityananda Senapati. "The effect of mass transfer on MHD free convective radiating flow over an impulsively started vertical plate embedded in a porous medium." *J. Appl. Anal. Comput* 5 (2015): 18-27. https://doi.org/10.11948/2015002

[22] Chiam, T. C. "Magnetohydrodynamic heat transfer over a non-isothermal stretching sheet." *Acta Mechanica* 122, no. 1-4 (1997): 169-179. https://doi.org/10.1007/BF01181997

[23] Abel, M. Subhas, Emmanuel Sanjayanand, and Mahantesh M. Nandeppanavar. "Viscoelastic MHD flow and heat transfer over a stretching sheet with viscous and ohmic dissipations." *Communications in Nonlinear Science and Numerical Simulation* 13, no. 9 (2008): 1808-1821. https://doi.org/10.1016/j.cnsns.2007.04.007

[24] Chen, Chien-Hsin. "Combined heat and mass transfer in MHD free convection from a vertical surface with Ohmic heating and viscous dissipation." *International journal of engineering science* 42, no. 7 (2004): 699-713. https://doi.org/10.1016/j.ijengsci.2003.09.002

[25] Abo-Eldahab, Emad M., and Mohamed A. El Aziz. "Viscous dissipation and Joule heating effects on MHD-free convection from a vertical plate with power-law variation in surface temperature in the presence of Hall and ion-slip currents." *Applied Mathematical Modelling* 29, no. 6 (2005): 579-595. https://doi.org/10.1016/j.apm.2004.10.005

[26] Oke, Abayomi Samuel. "Combined effects of Coriolis force and nanoparticle properties on the dynamics of gold–water nanofluid across nonuniform surface." *ZAMM-Journal of Applied Mathematics and Mechanics/Zeitschrift für Angewandte Mathematik und Mechanik* 102, no. 9 (2022): e202100113. https://doi.org/10.1002/zamm.202100113

[27] Oke, Abayomi S., and Winifred N. Mutuku. "Significance of viscous dissipation on MHD Eyring–Powell flow past a convectively heated stretching sheet." *Pramana* 95, no. 4 (2021): 199. https://doi.org/10.1007/s12043-021-02237-3

[28] Oke, Abayomi S., Winifred N. Mutuku, Mark Kimathi, and Isaac Lare Animasaun. "Coriolis effects on MHD newtonian flow over a rotating non-uniform surface." *Proceedings of the Institution of Mechanical Engineers, Part C: Journal of Mechanical Engineering Science* 235, no. 19 (2021): 3875-3887. https://doi.org/10.1177/0954406220969730

[29] Ouru, J. O., W. N. Mutuku, and A. S. Oke. "Buoyancy-induced MHD stagnation point flow of Williamson fluid with thermal radiation." *Journal of Engineering Research and Reports* 11, no. 4 (2020): 9-18. https://doi.org/10.9734/jerr/2020/v11i417065

[30] Bhargava, R., and Sonam Singh. "Numerical simulation of unsteady MHD flow and heat transfer of a second grade fluid with viscous dissipation and Joule heating using meshfree approach." *World Academy of Science, Engineering and Technology* 66 (2012): 1215.

[31] Singh, Ajay Kumar, and Rama Subba Reddy Gorla. "Free convection heat and mass transfer with Hall current, Joule heating and thermal diffusion." *Heat and Mass Transfer* 45 (2009): 1341-1349. https://doi.org/10.1007/s00231-009-0506-9

[32] Juma, Belindar A., Abayomi S. Oke, Winifred N. Mutuku, Afolabi G. Ariwayo, and Olum J. Ouru. "Dynamics of Williamson fluid over an inclined surface subject to Coriolis and Lorentz forces." *Engineering and Applied Science Letter* 5, no. 1 (2022): 37-46.

[33] Reddy, K. Veera, G. Venkata Ramana Reddy, A. Sandhya, and Y. Hari Krishna. "Numerical solution of MHD, Soret, Dufour, and thermal radiation contributions on unsteady free convection motion of Casson liquid past a semi-infinite vertical porous plate." *Heat Transfer* 51, no. 3 (2022): 2837-2858. https://doi.org/10.1002/htj.22452

[34] Oke, A. S. "Convergence of differential transform method for ordinary differential equations." *Journal of Advances in Mathematics and Computer Science* 24, no. 6 (2017): 1-17. https://doi.org/10.9734/JAMCS/2017/36489

[35] Rashidi, Mohammad Mehdi, Behnam Rostami, Navid Freidoonimehr, and Saeid Abbasbandy. "Free convective heat and mass transfer for MHD fluid flow over a permeable vertical stretching sheet in the presence of the radiation and buoyancy effects." *Ain Shams Engineering Journal* 5, no. 3 (2014): 901-912. https://doi.org/10.1016/j.asej.2014.02.007

[36] Thumma, Thirupathi, and M. D. Shamshuddin. "Buoyancy ratio and heat source effects on MHD flow over an inclined non-linearly stretching sheet." *Frontiers in Heat and Mass Transfer (FHMT)* 10 (2018). https://doi.org/10.5098/hmt.10.5